Desalination and Water Treatment
www.deswater.com

doi: 10.5004/dwt.2019.23786

156 (2019) 229–237
July

Development and study of sandwiched layer ceramic membrane

Avirup Saha, Monal Dutta*

Department of Chemical Engineering, Calcutta Institute of Technology, West Bengal – 711316, India, email: 96.avirupsaha@gmail.com (A. Saha), soniairin@gmail.com (M. Dutta)

Received 19 July 2018; Accepted 12 January 2019

ABSTRACT

Phenol is a harmful water pollutant affecting human health. Thus removal of phenol is important for water treatment. The present research aims at the development, characterization and application of a sandwiched layer ceramic membrane for removal of phenol from aqueous solution. The membrane was developed using inexpensive river clay through paste casting technique at 980°C. The membrane was characterized by Brunauer Emmett Teller (BET) apparatus (Autosorb-1, Quantacrome, USA), field emission scanning electron microscope (FESEM, JEOL JSM-7610F with EDS module), X-ray diffraction (XRD) analysis and Fourier transform infrared spectroscopy (FTIR, Perkin Elmer, USA). The BET surface area (S_{BET}, m^2/g) and average pore size (d_{Avg}, Å) of the crushed membrane were determined as 0.89 m^2/g and 84 Å respectively. The porosity of the casted membrane was calculated as 43% using water. The average pore size of the membrane was found to be 9.96 µm measured using water whereas, the pure water permeability was found to be 1×10^{-6} m/s-kPa. The porosity values measured by BET and water might differ due to the particle size, fluid used and applied pressure. The compressive strength of the membrane was calculated as 2.33 MPa. The membrane was employed for the removal of phenol at varying applied pressure (196–392 kPa), initial concentration (30–120 mg/L) and cross flow rate (0.08×10^{-7}–2.4×10^{-6} m^3/s). A significant enhancement of the permeate flux was observed from 792 to 1008 LMH (2.2×10^{-4} to 2.8×10^{-4} m^3/m^2-s) with increase in applied pressure from 196 to 392 kPa for a feed concentration 100 mg/L due to the increase in driving force. The cost of the membrane was evaluated and found to be around Rs. 19 for a single membrane.

Keywords: Ceramic membrane; Phenol; Microfiltration; Driving force; Cost

1. Introduction

The application of membrane technology for separation of various hazardous chemicals from industrial wastewater has gained immense importance in the present decade [1]. Among different existing commercial processes, the membrane separation techniques such as microfiltration, ultrafiltration, reverse osmosis, nanofiltration are widely employed for the removal of solid particles, microorganisms and colloidal materials from a given sample [2]. Generally most of the commercial membranes are developed from polymeric base materials and hence they are not susceptible to extreme process conditions [3]. In order to overcome this difficulty, ceramic membranes are often used. They have good thermal and chemical stability and long lifetime [4–6]. As most of the ceramic membranes are prepared from inexpensive precursor materials such as, clay [7], fly ash [8], phosphate [9] etc they offer the advantage of economical viability. So far, many researchers had developed tubular and supported ceramic membrane from different raw materials. A tubular membrane was developed from Moroccan perlite [10]. On the other hand, cordierite and natural clay material were used as membrane support to develop microfiltration and ultrafiltration membranes respectively [11]. Synthetic phosphates and silicates were also employed to develop ceramic membranes [12,13]. Among all these precursor materials, the use of clay mate-

*Corresponding author.

Presented at the InDA Conference 2018 (InDACON-2018), 20–21 April 2018, Tiruchirappalli, India

1944-3994 / 1944-3986

rials for casting of ceramic membranes is widely practiced as they are abundantly available and offer better mechanical strength even after sintering at lower temperature [14]. Other advantages of using clay materials are high surface area and porous structure for which they are widely used as adsorbent materials [15,16]. Considering all these physical factors, development of ceramic membranes from different clay materials has been identified as an emerging area of research especially in developing countries where economical viability is a serious concern. This approach also helps to address the environmental challenges caused due to the disposal of the used adsorbent materials. In the present study, inexpensive river clay has been used to fabricate a sandwiched layer ceramic membrane which was employed to remove phenol from aqueous solution. The advantage of using sandwiched layer membrane is to ensure the better adsorption of the pollutant by enhancing the residence time.

2. Experimental

2.1 Membrane preparation

2.1.1. Casting of membrane

In the present study, the ceramic membrane was prepared through paste casting technique by using the clay collected from local river basin of Ganges, sodium hydroxide (Rankem, Thane, India, AR grade, 97% purity), sodium nitrate (Nice Chemicals, Kerala India, LR grade, 98% purity), oxalic acid (Rankem, Thane, India, AR grade, 99.5% purity) and activated carbon (Merck Specialities Pvt. Ltd., Mumbai, India) in predetermined proportion. Here, the river clay, sodium nitrate and oxalic acid were mixed in different proportions with distilled water in order to form the outer and inner layers. It may be noted that double distilled water was used in this work.

For fabrication of the outer skin layers, 15 g soil was treated with 3 M NaOH solution followed by addition of sodium nitrate and oxalic acid at an impregnation ratio of 0.15 (w/w) each. On the other hand the inner layers of the sandwiched membrane were prepared by mixing 20 g of soil with sodium nitrate and oxalic acid at an impregnation ratio of 0.1 (w/w) using 1 M NaOH solution. The membranes (Fig. 1) were cast in five subsequent layers such as two outer skin layers and two inner layers with one carbon layer sandwiched between the two inner layers. The sandwich membrane was prepared in the shape of a circular disc of 75 mm diameter and 0.6 cm thickness. Then it was kept in room temperature for 12 h for drying and finally it was subjected to control heating in a programmable muffle furnace (Electronics and Electrical Engineering Co., Kolkata, India) up to 980ºC. A similar kind of fabrication process was adopted in a previous study by the research group to develop a chalk layered ceramic membrane [17].

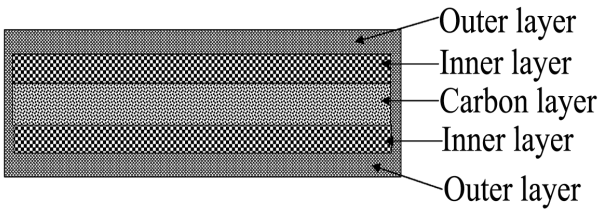

Fig. 1. Schematic of the membrane.

2.1.2. Sintering of ceramic membrane

Eventually, the casted membrane was heated in a programmable muffle furnace (Electronics and Electrical Engineering Co., Kolkata, India) at a predefined rate (2.22°C/min for 1.5 h, then 4.67°C/min for 1.25 h followed by 5.73°C/min until 980ºC). The rate of heating was slowly increased to avoid the formation of cracks. Then the membrane was soaked at 980ºC for 30 min to provide structural strength. It was cooled to room temperature inside the muffle furnace. Finally, the membrane was polished with silicon carbide abrasive paper (C-180) to give a nice look and have the final dimensions of 75 mm diameter and 0.6 cm thickness with a smooth surface.

2.2. Characterization of prepared membrane

The prepared membrane was characterized by Brunauer Emmett Teller (BET) apparatus (Autosorb-1, Quantacrome, USA) and Fourier transform infrared spectroscopy (FTIR, Perkin Elmer, USA). The BET surface area (S_{BET}, m^2/g), total pore volume (V_{tot}, cc/g) and average pore size (d_{Avg}, Å) were determined from the physical adsorption data of N_2 at 77 K with the help of BET equation for crushed membrane powder. The X-ray diffraction (XRD) analysis was carried out to identify the major components present in the membrane matrix. The XRD profile was measured by Oxford Instruments using Cu-Kα radiation source. The profile was recorded between angle 2θ of 10–80º with a scan rate of 0.08°/s and a generator voltage of 45 V. The surface morphology of a small sample of the membrane was characterized using a field emission scanning electron microscope (FESEM, JEOL JSM-7610F). The sample was coated with gold using sputtering technique prior to analysis. The porosity of the prepared membrane was studied through water permeability test. The compressive strength of the prepared membrane was determined by a compressive strength testing machine (TEST MASTER, Kolkata).

2.3. Design of filtration system

A portable home-made filtration setup was fabricated to study the flux of molecules through solvent permeation experiments. The schematic of the experimental set up is shown in Fig. 2.

The feed holdup chamber was made up of a perspex (polymethyl methacrylate) tube of 79 mm diameter and 140 mm length. The holding capacity of the chamber was found to be 685 mL. At the bottom of the chamber a supporting base plate was fixed on which the membrane was placed in a way that there was no leak from the sides. Inside the cylindrical compartment compressed air was supplied at a specified pressure (196–392 kPa) and flow rate (0.75 LPM) to enhance permeation efficacy.

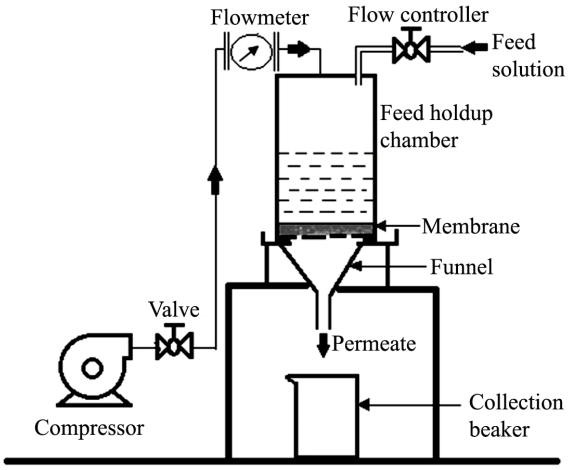

Fig. 2. Schematic of experimental setup.

2.3.1. Measurement of water flux

The holdup chamber was filled with measured quantity of water. The water was allowed to penetrate through the membrane pores at different applied pressure ranging from 196–392 kPa. The water flux going out through the membrane was measured as a function of time. The pressure was varied by using a bypass valve starting from lowest to highest pressure. The pure water flux (J_w) was determined using the following expression [18]

$$J_w = \frac{Q}{At} \tag{1}$$

where Q is the permeate water volume in mL and A is the membrane area in m^2 and t is time required in second.

2.3.2. Filtration of phenol containing water

In the present study, the filtration experiment was carried out at ambient temperature (25°C) (Fig. 2). Prior to the experiment with phenol contaminated water, distilled water was allowed to pass through the membrane under applied pressure in order to remove the loose particles blocking the pores of the membrane. The stock solution was prepared by dissolving required amount of phenol in distilled water and then the stock solution was subsequently diluted by distilled water to prepare solutions of various phenol concentrations ranging from 30–120 mg/L. The filtration study was carried out for a time period of 30 min at various operating conditions such as applied pressure of 196–392 kPa, feed concentrations of 30–120 mg/L and cross flow rates of 0.08×10^{-7}–2.40×10^{-6} m^3/s.

The observed rejection (%R) of the prepared membranes was determined by the following expression

$$\%R = \frac{C_0 - C_p}{C_0} \times 100 \tag{2}$$

where C_0 is the feed concentration and C_p is the permeate concentration in mg/L. The aliquots of the permeate samples were collected at regular time intervals and the samples were analyzed by using a UV-Vis spectrophotometer (Chemito, Spectrascan 2600) at a wave length of 270 nm.

3. Results and discussion

3.1. Characterization of developed ceramic membrane

3.1.1. BET analysis

The BET surface area (S_{BET}), total pore volume (V_{tot}) and average pore size of the crushed membrane was obtained from the physical adsorption data of N_2 at 77 K. The specific surface area and average pore size were found to be 0.89 m^2/g and 84 Å respectively. In order to elucidate the existence of micro and mesopores on the adsorbent surface, density function theory (DFT) was applied. The pore volume distribution curve is shown in Fig. 3. It is observed from Fig. 3 that a major peak is present at around 53 Å which indicates the presence of mesopores on the adsorbent surface [19].

3.1.2. Fourier transform infrared spectroscopy analysis

In order to confirm the presence of various functional groups on the adsorbent surface FTIR spectral analysis (Fig. 4) was performed using finely crushed membrane. Different functional groups containing oxygen are found to be present on the adsorbent surface corresponding to various spectrum bands [20]. The shift of peak positions due to adjacent groups and overlap of peaks make the FTIR analysis of clay components a bit complex. Table 1 summarizes the results of FTIR analysis.

3.1.3. X-ray diffraction analysis

The XRD pattern of the crushed membrane is shown in Fig. 5. The sharp peaks denote the presence of significant amount of crystalline phase in the prepared membrane. The XRD pattern identifies the presence of various compounds such as mullite ($3Al_2O_3$ $2SiO_2$), quartz (SiO_2), illite and kaolin [29].

3.1.4. Surface morphology

In order to investigate the surface and internal morphology, FESEM images of the surface, cross-section and small particle of the membrane (Figs. 6a, b and c respectively) were taken. Blocks were cut from the membrane to study the surface and cross-section. The blocks were placed in moulds and fixed with epoxy resin. The surfaces were then polished using different particle size of diamond pastes. Struers Polisher was used to create a scratch-free surface. The polished samples were sputter-coated with a palladium/gold layer to have an electrically conductive surface. A section of the membrane was crushed to small particle size and placed on a double-sided adhesive coated copper strip. The particles sticking to the copper strip were then coated with palladium/gold layer and used for analysis.

The FESEM image reveals the consistency and porous structure of the membrane surface. The FESEM of the surface (Fig. 6a) shows the presence of pores. The cross-section (Fig. 6b) shows a network of rod-like structure with some smaller particles filling the spaces creating a network of pores. The rod-like structures are more prominent in the cross-sectional view. The analysis of the small particles

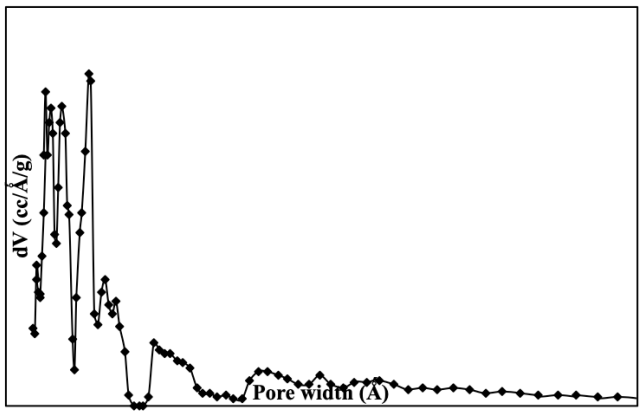

Fig. 3. The DFT pore size distribution curve of the crushed membrane.

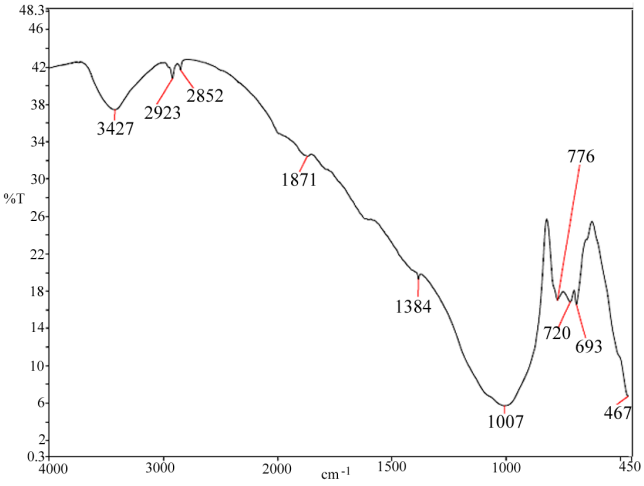

Fig. 4. The FTIR spectra of crushed membrane.

Table 1
Summary of FTIR peaks

FTIR peak, cm^{-1}	Functional group	Associated compounds present in clay	References
720	AlO_6	Kaolin, mullite	[21]
1007	Si-O stretching	SiO_2	[22]
776	Si-O Stretching	SiO_2, Clay	[23]
3427	Stretching bands of the structural OH	Montmorillonite	[24]
693	Si-O stretching	SiO_2	[25,26]
467	Si–O–Si bending vibrations	Silica	
1384,	γ-Al_2O_3	Alumina	[27]
1871	Quartz overtone	Silica	
2852, 2922,	Aliphatic C-H stretching	Organic matter	[28]

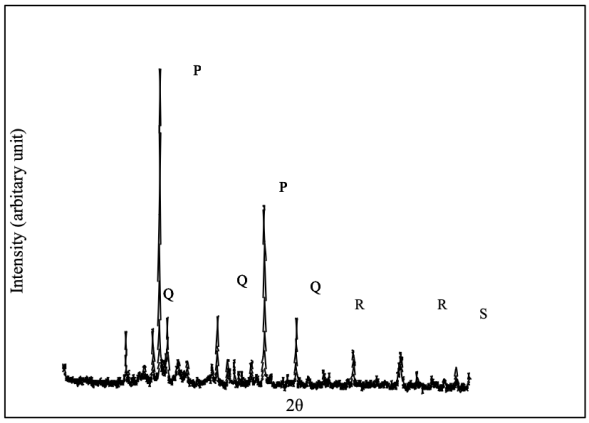

Fig. 5. XRD patterns of crushed membrane (P-mullite, Q-quartz, R-kaolin, S-illite).

indicates presence of pores. The overall morphology of the membrane surface suggests the absence of cracks and deformities and presence of meso and macro pores indicating the characteristics of a good membrane [30].

3.1.5. Porosity determination

As the membrane will finally be used for removal of phenol from aqueous solution it is important to analyze the porosity with respect to water of the fabricated membrane (without crushing). The membrane was weighed initially (Wi) by dipping in water for a significant time. Then the surface was cleaned by absorbent paper so that the surface becomes dry. The wet membrane was weighed (W_f) again. Thus volume of water absorbed was measured by dividing ($W_f - W_i$) by the density of water. The volume of the membrane was measured based on its physical dimensions. The porosity of the membrane was calculated by dividing the volume of absorbed water by the volume of the membrane. It was assumed that the volume of the water absorbed represented the pore volume as water entered into the pores. In this investigation, the average porosity of the membrane was found to be 43%. Similar result was also obtained in the previous literature [31]. It may be noted that in BET based porosity measurement of the crushed membrane nitrogen gas at high pressure was used while the porosity of the membrane was measured using water under atmospheric pressure. It was not possible to measure the porosity of the fabricated membrane without crushing using BET apparatus due to the sample size limitation of the equipment. The measurement of porosity gets influenced by the fluid used, particle size of the sample, the wettability of the sample by the fluid and the applied pressure. The porosity of the membrane was created partly by the passage of carbon-dioxide due to breaking of bonds of oxalic acid during heating. As the membrane was sintered placing the sample on a refractory plate it is possible that the release of carbon-dioxide might have some directional nature resulting in higher porosity at the top surface compared to that at the bottom surface. However the focus was on the measurement of average porosity as it is difficult to measure the porosity distribution with height due to the small thickness of the membrane.

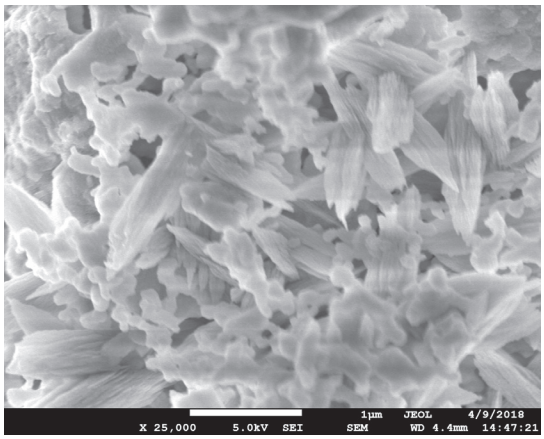

(a)

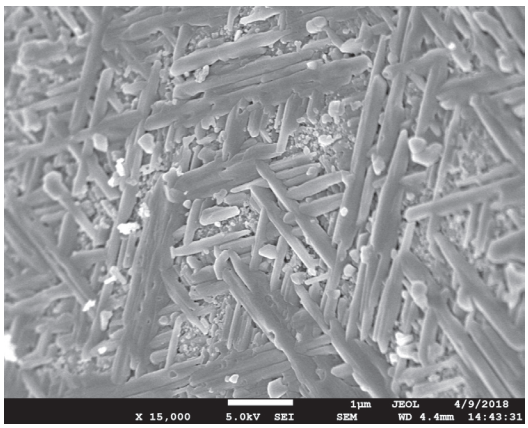

(b)

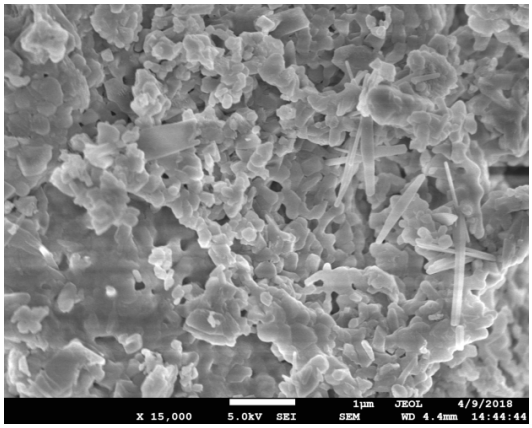

(c)

Fig. 6. FESEM image of the prepared membrane (a) Surface, (b) Cross-section and (c) Small particle.

3.1.6. Water permeability test

The water flux was determined as a function of time at different applied pressures varied from 196–392 kPa. The steady state permeability was attained over the experimental time. The variation of water flux as a function of time at various applied pressures is plotted in Fig. 7. It can be seen from Fig. 7 that the steady flux is achieved over the entire length of time starting from 20 s. Each experiment was repeated thrice and the average values were plotted. The error bars were plotted based on standard deviation.

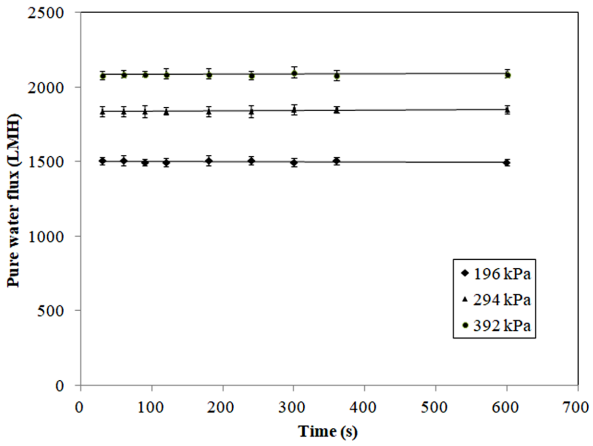

Fig. 7. The pure water flux as a function of time.

The increase in applied pressure increased the trans-membrane pressure drop. Fig. 7 shows that increase in applied pressure resulted in an increase in water flux. This may be due to increase in driving force due to increase in trans-membrane pressure drop. As the primary transport mechanism across the membrane surface is convection, therefore increase in water flux (J_w) with increase in driving force can directly be linked up with Darcy's law. Thus the water permeability (L_p) of the membrane was determined using the following equation [32].

$$J_w = L_p \Delta P \tag{3}$$

It may also be noted that increase in water flux is more prominent at higher pressure. Thus the average water permeability for the experimental pressure range was calculated as an approximation. The average water permeability was found to be around 1×10^{-6} m/s-kPa based on the slope of the linear plot of J_w against applied pressure (R^2 value of 0.84). Hagen-Poiseuille equation was combined with Darcy's law to determine the average pore size by using the following expression [33].

$$r = \left[\frac{L_p 8\mu\tau l}{\varepsilon} \right]^{1/2} \tag{4}$$

where ε is the porosity of the developed membranes (0.43); r is the pore radius of the membrane (m); l is the pore length (0.006 m) which is generally taken as thickness of the membrane; τ is the tortuosity factor (generally used as 1); μ is the viscosity of water (0.00089 Pa-s).

Therefore, by using this correlation [Eq. (4)] the pore radius of the prepared membrane was calculated as 9.96 μm which lies in the range of microfiltration membrane. This average pore size of the membrane differed from that measured by BET apparatus due to the particle size of the sample, the fluid and measurement conditions.

3.1.7. Determination of compressive strength

The compressive strength of the developed membrane was found to be 2.33 MPa and this result is in good agreement with previous literature [34]. It may be noted that during use of the membrane no powder dropping or abrasion was observed. Due to sintering the ceramic membrane gained strength and stability.

Finally, the overall membrane properties are summarized in Table 2. The values are in good agreement with published works and can be suitable for various industrial applications. It may also be noted that the membrane has been prepared at a temperature below 1000ºC which might encourage industries to go for it.

3.2. Application of developed membrane in phenol-water system

The developed disk shaped ceramic membrane was used to study the removal of phenol from aqueous solution. The permeation flux and the percent rejection of the membrane was evaluated as a function of time at varying pressure and feed concentrations. These effects are discussed in the following sections.

3.2.1. Effect of applied pressure on permeate flux and percent rejection

The effect of applied pressure on permeate flux was studied at a cross flow rate of 2.4×10^{-6} m^3/s with an initial feed concentration of 100 mg/L as shown in Fig. 8. Initially a steep decline in the permeation flux was observed. However, the flux gradually subsided with time. This may be attributed to concentration polarization on the membrane surface due to increasing thickness of mass transfer boundary layer and partial pore blocking [35]. Besides, it is observed from Fig. 8 that with increase in applied pressure the permeate flux increases due to increase in driving force as prescribed by Darcy's law. Each experiment was repeated thrice and the average values were plotted. The error bars were plotted based on standard deviation.

The change in permeate flux with increase in applied pressure is shown as an inset of Fig. 8. The nature of this curve is not linear and this may be due to concentration polarization above the membrane surface [36]. Besides, the rate of decrease in permeate flux is higher at higher applied pressure due to membrane fouling.

The percent rejection of the developed membrane at varying applied pressures for initial feed concentration of 100 mg/L is shown in Fig. 9. The calculation for Fig. 9 was made based on the average of the three measurements shown in Fig. 8. Here the cross flow rate was fixed at 2.4×10^{-6} m^3/s. It can be seen from this figure that phenol rejection declines with increase in applied pressure as at increased pressure some of the phenol molecules are forced towards the permeate side [37]. Moreover, the percent rejection of membranes is found to increase by a small amount with the progress of time (after 250 s) due to adsorption of phenol molecules in the pore interiors. According to Fig. 9, the fabricated membrane exhibited good rejection percentage of 99.74% at an applied pressure of 196 kPa with an initial concentration of 100 mg/L.

Table 2
Properties of developed ceramic membrane

Parameter	Value
Membrane diameter (mm)	75
Average pore diameter (from H_2O permeability)	9.96 µm
Porosity	0.43
Water permeability (m^3/m^2-kPa-s)	1×10^{-6}
Compressive strength (MPa)	2.33

3.2.2. Effect of feed concentration on permeate flux and percent rejection

In order to study the effect of initial phenol concentration on permeate flux and percent phenol rejection, the

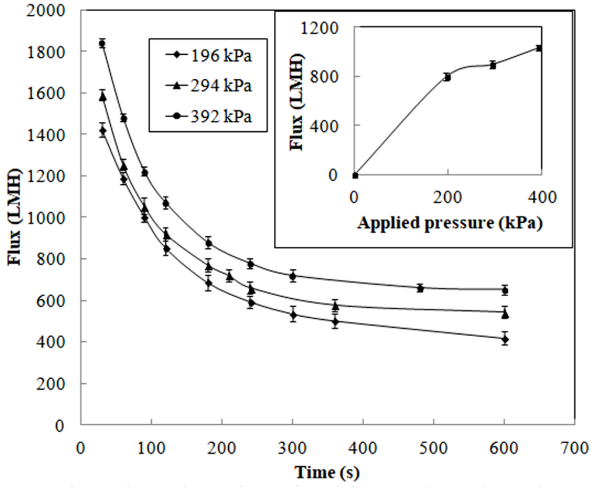

Fig. 8. Effect of applied pressure on permeate flux for an initial feed concentration of 100 mg/L.

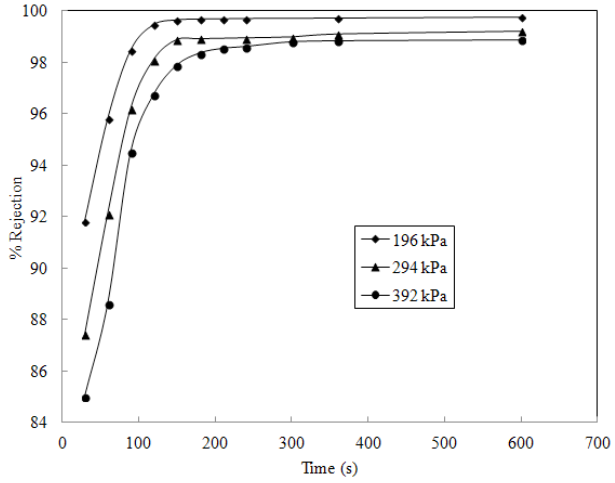

Fig. 9. Effect of applied pressure on percent rejection for an initial feed concentration of 100 mg/L.

permeate flux and percent phenol rejection were plotted as a function of time at varying feed concentrations (Figs. 10 and 11). The applied pressure and the cross flow rate were maintained at 392 kPa and 2.4×10^{-6} m^3/s respectively. Each experiment was repeated thrice and the average values were plotted. The error bars were plotted based on standard deviation. It is evident from Fig. 10 that with increase in feed concentration the permeate flux decreases as at higher concentration there is more chances of membrane fouling due to deposition of solute molecule on the membrane surface as well as in the pore interior resulting in decreased permeate flux [38]. The decrease in permeate flux may also happen due to coalescence of solute molecules [39].

The effect of feed concentration on percent rejection was also investigated (Fig. 11). The calculation for Fig.11 was made based on the average of the three measurements shown in Fig. 10. It is evident from Fig. 11 that percent rejection increased from 81.02 to 99.78% for high initial feed concentration of 100 to 120 mg/L at an applied pressure of 392 kPa. The increase in percent rejection was much higher with low initial feed concentration (30 mg/L). However, in this case the equilibrium value was lower compared to that for higher initial feed concentration. The probable reason may be at higher feed concentration coalescence of solute molecule took place which enhanced the percent rejection [40].

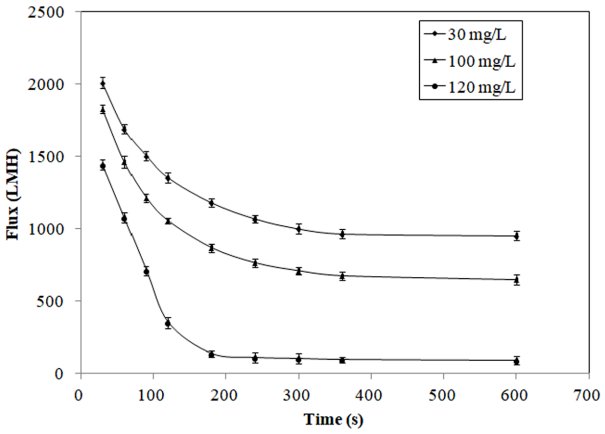

Fig. 10. Effect of feed concentration on permeate flux at 392 kPa.

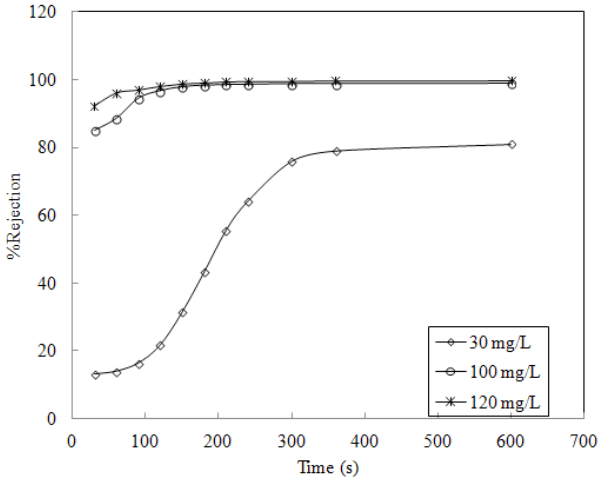

Fig. 11. Effect of feed concentration on percent rejection at 392 kPa.

3.2.3. Effect of cross flow rate on permeate flux and percent rejection

The effects of cross flow rate on permeate flux (Fig. 12) and percent rejection (Fig. 13) were evaluated at an applied pressure of 392 kPa and with a feed concentration of 100 mg/L. The cross flow rates were varied from 0.08×10^{-7} to 2.4×10^{-6} m^3/s. It was found that the permeate flux increased with an increase in cross flow velocity. The possible reason may be at increased cross flow rate the value of mass transfer coefficient increased which in turn reduced the effect of concentration polarization [41]. Each experiment was repeated thrice and the average values were plotted. The error bars were plotted based on standard deviation.

The variation in percent rejection with varying cross flow rate is depicted in Fig. 13. The calculation for Fig.13 was made based on the average of the three measurements

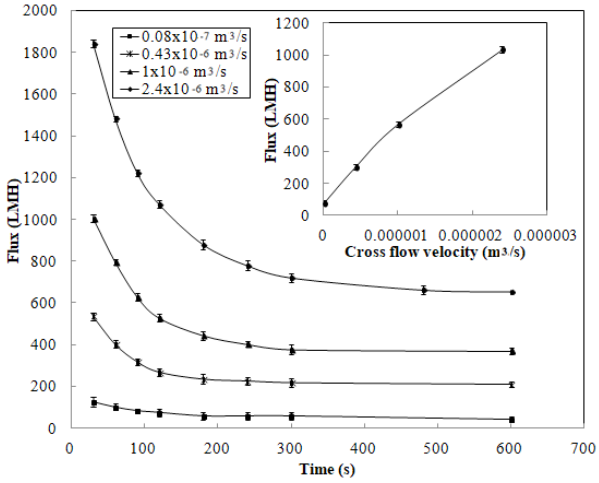

Fig. 12. Effect of cross flow rate on permeate flux at 392 kPa.

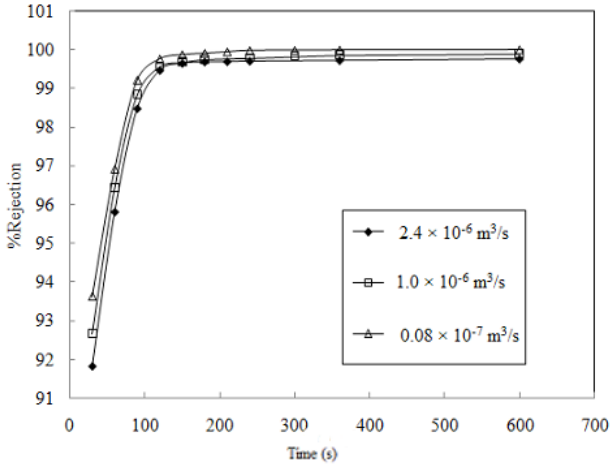

Fig. 13. Effect of cross flow rates on percent rejection at 392 kPa.

Table 3
Cost analysis of a single membrane

Raw materials	Cost/500 g (INR)	Amount required (g)	Cost of raw materials (INR)
Clay			0.07
Oxalic acid	219.00	6	2.63
Sodium nitrate	240.00	0.5	0.24
Sodium Hydroxide	314.00	11.68	7.33
Activated carbon	438.00	10	8.76
Total cost for single membrane (INR)			19.00 (approx)

shown in Fig. 12. The percent rejection values decreased slightly with increase in cross flow velocity due to reduced thickness of mass transfer boundary layer over the membrane surface at high feed concentration leading to better rejection [42]. Therefore, the chances of formation of cake layer which acts as a barrier is significantly reduced at higher flow rates resulting in decreased rejection. Here the percent rejection declined from 99.98 to 99.74% with increase in cross flow rate from 0.08×10^{-7} to 2.4×10^{-6} m^3/s.

3.3. Cost estimation of membrane

The authors have reported the fabrication and use of low-cost ceramic membranes [43,44] for removal of contaminants from aqueous solution. In the present study, a ceramic membrane has been fabricated for removal of phenol from water. The cost of the developed ceramic membrane is determined on the basis of raw materials used and it is estimated to be around Rs. 19/membrane as shown in Table 3. The raw materials cost of the membrane per unit area is estimated to be Rs. 2040/m^2 (30.66 \$/m^2). On the other hand, the cost of other inorganic membranes is found to be approximately 500–1000\$/m^2 [45] whereas, the polymeric membrane costs approximately 50–200\$/m^2 [46]. Therefore, it can be said from the cost estimation that the prepared membrane is inexpensive as compared to commercial membranes, based on the sintering temperature and raw materials utilized in this study.

4. Conclusions

In the present investigation microfiltration membrane was developed from locally available river clay collected from the basin of Ganges through paste casting technique. During the casting technique, the paste was prepared by mixing various precursor materials such as river clay, sodium nitrate, oxalic acid and commercial activated carbon in different proportions by using NaOH solution of varying strength (1 M and 3 M). The addition of small amount of oxalic acid increased the membrane porosity by few folds whereas sodium hydroxide provided the membrane strength by lowering the sintering temperature. Once the paste was prepared it was casted over a metal plate in the form of a circular disk of 75 mm diameter and then placed inside a muffle furnace for sintering. The membrane was sintered at 980°C at a controlled heating rate and kept at this temperature for 30 min for soaking.

The crushed membrane was characterized by BET equipment, FTIR and XRD. The prepared membrane was characterized via FESEM analysis and porosity measurement using water. A crystalline structure was observed in the XRD image. The absence of cracks and deformities were also confirmed from the FESEM image. The pure water flux values were also checked for the prepared membrane and the value was found to be 1×10^{-6} m/s-kPa whereas the porosity was also calculated as 0.43. The pore size from the pure water permeability was evaluated as 9.96 μm for the prepared membrane which lies in the microfiltration region. However the pore size differed from that obtained by BET equipment for crushed membrane (84 Å). The compressive strength of the membrane was determined as 2.33 MPa.

The prepared membrane was utilized to remove phenol from aqueous solution through microfiltration system at varying experimental conditions. The permeate flux and percent rejection of the developed membrane were plotted as a function of time and applied pressure for varying feed concentrations and cross flow rates. It was observed that the permeate flux increased from 792 to 1008 LMH (2.2×10^{-4} to 2.8×10^{-4} m^3/m^2-s) with increase in applied pressure from 196 to 392 kPa for a feed concentration 100 mg/L due to increase in driving force. On the other hand, a visible decline in permeate flux from 792 to 97.2 LMH (2.2×10^{-4} to 2.7×10^{-5} m^3/m^2-s) was observed as the feed concentration was increased from 30 to 120 mg/L due to growing thickness of concentration boundary layer.

Finally the cost of the prepared membrane was evaluated and it was found to be around Rs. 19 for a single membrane. Therefore, it can be concluded that in the present work a low cost ceramic membrane was produced from inexpensive precursor materials and the membrane can be utilized to remove phenol through microfiltration.

References

[1] R.D. Colle, C. Fortulan, S.R. Fontes, Manufacture and characterization of ultra and microfiltration ceramic membranes by isostatic pressing, Ceram. Int., 37 (2011) 1161–1168.
[2] C. Gaucher, P. Jaouen, J. Comiti, P. Legentilhomme, Determination of cake thickness and porosity during cross-flow ultrafiltration on a plane ceramic membrane surface using an electrochemical method, J. Membr. Sci., 210 (2002) 245–258.
[3] A. Harabi, F. Zenikheri, B. Boudaira, F. Bouzerara, A. Guechi, L. Foughali, A new and economic approach to fabricate resistant porous membrane supports using kaolin and $CaCO_3$, J. Eur. Ceram. Soc., 34 (2014) 1329–1340.
[4] R.D. Sahnoun, S. Baklouti, Characterization of flat ceramic membrane supports prepared with kaolin-phosphoric acid-starch, Appl. Clay Sci., 83–84 (2013) 399–404.
[5] S. Jana, M.K. Purkait, K. Mohanty, Preparation and characterization of low-cost ceramic microfiltration membranes fort the removal of chromate from aqueous solution, Appl. Clay Sci., 47 (2010) 317–324.
[6] H.J. Yeom, S.C. Kim, Y.W. Kim, I.H. Song, Processing of alumina-coated clay diatomite composite membranes for oily wastewater treatment, Ceram. Int., 42 (2016) 5024–5035.
[7] H. Elomari, B. Achiou, M. Ouammou, A. Albizane, J. Bennazha, S. Alami-Younssi, I. Elamrani, Elaboration and characterization of flat membrane supports from Moroccan clays. Application for the treatment of wastewater, Desal. Water Treat., 57(43) (2016) 20298–20306.

[8] J. Fang, G. Qin, W. Wei, X. Zhao, L. Jiang, Elaboration of new ceramic membrane from spherical fly ash for microfiltration of rigid particle suspension and oil-in water emulsion, Desalination, 311 (2013) 113–126.
[9] M. Khemakhem, S. Khemakhem, S. Ayedi, R. Ben Amar, Study of ceramic ultrafiltration membrane support based on phosphate industry sub product: application for the cuttlefish conditioning effluents treatment, Ceram. Int., 37 (2011) 3617–3625.
[10] A. Majouli, S. Tahiri, S. Alami-Younssi, H. Loukili, A. Albizane, Elaboration of new tubular ceramic membrane from local Moroccan perlite for microfiltration process: application to treatment of industrial wastewaters, Ceram. Int., 38 (2012) 4295–4303.
[11] N. Saffaj, S. Alami-Younssi, A. Albizane, A. Messouadi, M. Bouhria, M. Persin, M. Cretin, A. Larbot, Elaboration and characterization of TiO_2–$ZnAl_2O_4$ ultrafiltration membranes deposited on cordierite support, Sep. Purif. Technol., 36 (2004) 107–114.
[12] I. Barrouk, S. Alami-Younssi, A. Kabbabi, M. Persin, A. Albizane, S. Tahiri, Elaboration and characterization of ceramic membranes made from natural and synthetic phosphates and their application in filtration of chemical pretreated textile effluent, J. Mater. Environ. Sci., 6(8) (2015) 2190–2197.
[13] J.H. Eom, H.J. Yeom, Y.W. Kim, I.H. Song, Ceramic membranes prepared from a silicate and clay-mineral mixture for treatment of oily wastewater, Clay Clay Miner., 63 (2015) 222–234.
[14] I. Jedidi, S. Khemakhem, A. Larbot, R. Ben Amar, Elaboration and characterization of fly ash based mineral supports for microfiltration and ultrafiltration membranes, Ceram. Int., 35 (2009) 2747–2753.
[15] M. Roulia, A. Alexandros, A. Vassiliadis, Sorption characterization of a cationic dye retained by clays and perlite, Microporous Mesoporous Mater., 116 (2008) 732–740.
[16] Q. Zhou, R.L. Frost, H. He, Y. Xi, Changes in the surfaces of adsorbed paranitrophenol on HDTMA organoclay—the XRD and TG study, J. Colloid Interface Sci., 307 (2007) 50–55.
[17] A. Sengupta, A. Saha, S. Roy, M. Mitra, R. Mallick, A. Denra, S. Adak, M. Dutta, Elaboration of different pore blocking model for phenol removal using disk shaped ceramic membrane, Int. J. Eng. Adv. Technol., 7(5) (2018) 24–27.
[18] B. Chakrabarty, A.K. Ghoshal, M.K. Purkait, SEM analysis and gas permeability test to characterize polysulfone membrane prepared with polyethylene glycol as additive, J. Colloid Interface Sci., 320(1) (2008) 245–253.
[19] F. Doulati Ardejani, K. Badii, N.Y. Limaee, S.Z. Shafaei, A.R. Mirhabibi, Adsorption of direct red 80 dye from aqueous solution onto almond shells: effect of pH, initia concentration and shell type, J. Hazard. Mater., 15 (2008) 730–737.
[20] A. Krueger, The structure and reactivity of nanoscale diamond, J. Mater. Chem., 18 (2008) 1485–1492.
[21] A.K. Chakraborty, Phase Transformation of Kaolinite Clay, Springer India, (2014), ISBN 978-81-322-1154-9.
[22] K.A. Saeed, H. Saeed, K.A. Kassim, H. Nur, Physico-chemical characterization of lime stabilized tropical kaolin clay, J. Teknol., (Sci. E.), 72 (2015) 83–90.
[23] J. Kann, Oil shale, Estonian academy, 19(1) (2002), ISSN 0208-189X.
[24] A. Kiros, A.V. Gholap, G.E. Gigante, Fourier transform infrared spectroscopic characterization of clay minerals from rocks of Lalibela churches, Ethiopia, Int. J. Phy. Sci., 8(3) (2013) 109–119.
[25] E.E. Georges-Ivo, Fourier transform infrared spectrophotometry and X-ray powder diffractometry as complementary techniques in characterizing clay size fraction of kaolin, J. Appl. Sci. Environ. Mgt., 9 (2005) 43–48.
[26] S. Dikmen, A. Gunay, B. Ersoy, I. Erol, Determination of equilibrium, kinetic and thermodynamic parameters of acid red 88 adsorption onto montmorillonittic clay, Environ. Eng. Manage. J., 4 (2015) 1097–1110.
[27] A. Tinti, V. Tugnoli , S. Bonora, O. Francioso, Recent applications of vibrational mid-Infrared (IR) spectroscopy for studying soil components: a review, J. Central Europ. Agricul., 16 (2015) 1–22.
[28] D. Mitev, R. Dimitrova, M. Spassova, Ch. Minchev, S. Stavrev, Surface peculiarities of detonation nanodiamonds in dependence of fabrication and purification methods, Diam. Relat. Mater., 16 (2007) 776–780.
[29] P. Monash , G. Pugazhenthi, Development of ceramic supports derived from low-cost raw materials for membrane applications and its optimization based on sintering temperature, Int. J. Appl. Ceram. Technol., 8 (2011) 227–238.
[30] S. Kanchapogu, G. Pugazhenthi, Cross flow microfiltration of oil-water emulsions using clay based ceramic membrane support and TiO_2 composite membrane, Egyp. J. Petrol., 26 (2017) 679–694.
[31] N. Saffaj, M. Persin, S.A. Younsi, A. Albizane, M. Cretin, A. Larbot, Elaboration and characterization of microfiltration and ultrafiltration membranes deposited on raw support prepared from natural Moroccan clay: application to filtration of solution containing dyes and salts, Appl . Clay Sci., 31 (2006) 110–119.
[32] E. Levänen, T. Mäntylä, Effect of sintering temperature on functional properties of alumina membranes, J. Eur. Ceram. Soc., 22 (2002) 613–623.
[33] M.C. Almandoz, J. Marchese, P. Pradanos, L. Palacio, A. Hernandez, Preparation and characterization of non-supported microfiltration membranes from alu-minosilicates, J. Membr. Sci., 241 (2004) 95–103.
[34] B.K. Nandi, R. Uppaluri, M.K. Purkait, Preparation and characterization of low cost ceramic membranes for microfiltration applications, Appl. Clay Sci., 42 (2008) 102–110.
[35] D. Ghosh, M.K. Sinha, M.K. Purkait, A comparative analysis of low-cost ceramic membrane preparation for effective fluoride removal using hybrid technique, Desalination, 327 (2013) 2–13.
[36] B. Chakrabarty, A.K. Ghoshal, M.K. Purkait, Ultrafiltration of stable oil-in-water emulsion by polysulfone membrane, J. Membr. Sci., 325 (2008) 427–437.
[37] B. Díaz-Reinoso, A. Moure, H. Domínguez, J.C. Parajó, Ultra- and nanofiltration of aqueous extracts from distilled fermented grape pomace, J. Food Eng., 91 (2009) 587–593.
[38] R. Bergamasco, L.C. Konradt-Moraes, M.F. Vieira, M.R. Fagundes-Klen, A.M.S. Vieira, Performance of a coagulation-ultrafiltration hybrid process for water supply treatment, Chem. Eng. J., 166 (2011) 483–489.
[39] X. Sun, C. Wang, Y. Li, W. Wang, J. Wei, Treatment of phenolic wastewater by combined UF and NF/RO processes, Desalination, 355 (2015) 68–74.
[40] L.H. Andrade, F.D.S Mendes, J.C. Espindola, M.C.S. Amaral, Nanofiltration as tertiary treatment for the reuse of dairy wastewater treated by membrane bioreactor, Sep. Purif. Technol., 126 (2014) 21–29.
[41] R. Jiraratananon, A. Chanachai, A study of fouling in the ultrafiltration of passion fruit juice, J. Membr. Sci., 111 (1996) 39–48.
[42] Z. Zhong, F. Xu, Y. Cao, Z. X. Low, F. Zhang, W. Xing, Purifying condensed water with ceramic ultrafiltration membranes, J. Chem. Technol. Biotechnol., 90(11) (2015) 2092–2099.
[43] M. Mitra, S. Adak, R. Mallick, S. Roy, A. Sengupta, A. Denra, A. Saha, M. Dutta, Development of chalk layered microfiltration ceramic membrane, Int. J. Adv. Res. Ideas Innov. Technol., 4(3) (2018) 23–26.
[44] S. Roy, A. Denra, A. Saha, M. Mitra, S. Adak, R. Mallick, A. Sengupta, M. Dutta, Evaluation of fouling mechanism of ceramic membrane for oil-water system, Int. J. Innov. Res. Sci. Eng. Technol., 7(6) (2018) 6692–6696.
[45] S.P. Nunes, K.V. Peinemann, Membrane Technology in the Chemical Industry, Wiley, New York, 2001.
[46] B.D. Bhide, S.A. Stern, A new evaluation of membrane processes enrichment of air. II. Effects of economic membrane properties, J. Membr. Sci., 62 (1991) 37–58.